25th ABCM International Congress of Mechanical Engineering
October 20-25, 2019, Uberlândia, MG, Brazil

COB-2019-1180
CONDENSATION AND NORMAL SHOCK WAVE LOCATION IN SUPERSONIC NOZZLES

Andrés F. Bolaños-Acosta
Claudio T-Rodrigues
Julián C. Restrepo-Lozano
José R. Simões-Moreira
SISEA-Alternative Energy System Lab.,Escola Politécnica, University of São Paulo
Av. Professor Mello Moraes, 2231 - Butantã, São Paulo - SP, 05508-030.
afb.acosta@usp.br, claudiotr@usp.br, restrepo@usp.br, jrsimoes@usp.br

Abstract. *One of the most promising techniques for gas dehydration is the supersonic separation, which consists of the expansion of a fluid in a convergent-divergent nozzle, as the temperature falls due to the isentropic expansion, condensation or solidification occurs. A theoretical quasi one- dimensional pure substance model is built from the residual thermodynamic property theory based on the Van der Waals and Peng-Robinson equations, allowing to determine the thermodynamic properties in the nozzle. Compressible flow relations are also implemented in order to obtain the isentropic expansion and normal shock location in the nozzle flow. Finally, the binodal, spinodal and Wilson lines are calculated for the Peng-Robinson equation aiming to determine the condensation shock for carbon dioxide. The results of the model are compared to the numerical data avalaible on the literature, having a good agreement in ideal and close to the critical fluid conditions.*

Keywords: *compressible flow, converging-diverging nozzle, cubic EoS, gas dehydration.*

1. INTRODUCTION

Nowadays, natural gas is one of the most important sources of energy in the world (Haghighi *et al.*, 2013), raw natural gas is not a saleable product because it contains a blend of various hydrocarbonic gases, liquids and solid contaminants (Liu *et al.*, 2014).

The presence of water in the raw gas is the most common undesirable component; this fact not only reduces the heating value of natural gas as fuel, but also leads to pipe blockage in gas facilities (Restrepo and Simões-Moreira, 2019).

For the previous reason, dehydration of raw gas is presented as an important goal in operational gas conditioning process (Niknam *et al.*, 2018), helping to avoid the problems that occurs in downstream such as condensation, liquid slugging, and controlling of gas heating value, removing water or heavy hydrocarbons from the gas (Niknam *et al.*, 2017).

Many researches have been focused on the development of new technologies to remove liquids from the gas phase, these dehydration methods are characterized by their huge investment, the complexity of the mechanical structure, the need of large facilities to be implemented and the damage caused by this equipment to the environment (Liu *et al.*, 2014). Due to these facts, the using of supersonic nozzles for gas dehydration is a new concept that has been growing in recent years (Haghighi *et al.*, 2013).

During a gas supersonic expansion; the enthalpy of inlet gas stream is transformed to kinetic energy through an isentropic transition along with a temperature drop, which causes the heavy fractions to be condensed due to nucleation (Niknam *et al.*, 2017).

Hence, compressible flow relations are implemented in a quasi one- dimensional model using two cubic equations-of-state (EoS): the Van der Waals (VdW) and Peng-Robinson (PR) ones. The VdW equation is employed to locate the normal shock wave due to the simplicity in its thermodynamic formulation, which allows to validate the algorithm in ideal and close to the fluid critical conditions. In a similar manner, the PR EoS is also implemented, aiming to locate the condensation shock during an isentropic expansion by applying fundamentals of the homogeneous nucleation theory, the construction of the binodal and spinodal curves.

2. THERMODYNAMIC ASPECTS

A cubic EoS, may be written in its generic form as (Smith *et al.*, 2006):

$$P = \frac{RT}{V-b} - \frac{a}{(V+\varepsilon b)(V+\sigma b)} \tag{1}$$

Where P is the gas pressure, V is the specific volume, T is the temperature, R is the ideal gas constant, a and b are fluid dependent-parameters and the terms ε and σ depend on each EoS Eqs. (2-3), for the VdW case:

$$\varepsilon = \sigma = 0 \tag{2}$$

For the PR equation:

$$\varepsilon = \sqrt{2} \quad \sigma = \sqrt{-2} \tag{3}$$

The VdW EoS is treated in its polynomial reduced form Eq. (4), due to its facility to be solved computationally using Numpy (Oliphant, 2006) (a package for scientific computing with Python) .

$$V_r^3 - \left(\frac{8T_r}{P_r} + 1\right) V_r^2 + \frac{9V_r}{3P_r} - \frac{1}{P_r} = 0 \tag{4}$$

Where P_r, V_r, T_r are the reduced forms of the pressure, volume and temperature, respectively. The PR EoS is also treated in its polynomial form as a function of the compressibility factor, as follows:

$$Z^3 + (B-1)Z^2 + \left(A - 2B - 3B^2\right)Z + \left(B^3 + B^2 - AB\right) = 0 \tag{5}$$

With:

$$A = \frac{aP}{(RT)^2} \tag{6}$$

$$B = \frac{bP}{RT} \tag{7}$$

Note that Eq. (4) and Eq. (5) have three solutions, when they find the phase change zone, the solution with the highest value corresponds to the gas solution chosen for all simulations in this work.

Thermodynamic properties such as enthalpy and entropy, are formulated based on their residual and ideal parts. To calculate the ideal contribution for both EoS is used the formulation given by Smith *et al.* (2006). The residual properties are estimated according to the procedure presented by Smith *et al.* (2006). For the VdW equation, the residual enthalpy and entropy are expresssed by the Eqs. (8) and (9) respectively.

$$h^R = -RT\left(\frac{2a}{RTV} - \frac{b}{V-b}\right) \tag{8}$$

$$s^R = R\ln\left\{Z\left(1 - \frac{b}{V}\right)\right\} \tag{9}$$

And for the PR EoS, the residual enthalpy and entropy are expresssed by the Eqs. (10) and (11) respectively.

$$h^R = \left\{Z - 1 - \left(\frac{A}{B\sqrt{8}}\right)\left(1 + \frac{k\sqrt{T_r}}{\sqrt{\alpha}}\right)\ln\left(\frac{Z + \left(1+\sqrt{2}\right)B}{Z + \left(1-\sqrt{2}\right)B}\right)\right\} RT \tag{10}$$

$$s^R = \left\{\ln\left(Z - B\right) - \left(\frac{A}{B\sqrt{8}}\right)\left(\frac{k\sqrt{T_r}}{\sqrt{\alpha}}\right)\ln\left(\frac{Z + \left(1+\sqrt{2}\right)B}{Z + \left(1-\sqrt{2}\right)B}\right)\right\} R \tag{11}$$

The terms k and α are also fluid-dependent parameters, detailed information about their calculation (including a and b) is reported by Smith *et al.* (2006), and the R superscript denotes residual property.

According to Eq. (12), the speed of sound is obtained following the procedure carried out by Pratt (2001) in which is expressed as a function of the derivatives for each EoS, the specific volume and the terms c_p and c_v (constant pressure and volume specific heats).

$$c = V\sqrt{-\frac{c_p}{c_v}\left(\frac{\partial P}{\partial V}\right)_T} \tag{12}$$

Where c is the speed of sound, the terms c_p, c_v and $(\partial P/\partial V)_T$ are calculated for each equation of state, detailed information about its calculation is available in the work developed by Pratt (2001). In order to calculate the thermodynamic properties, three computational functions are built in a Python script (Rossum, 1995), which are listed below:

- P-T solver: pressure and temperature as input pairs.
- P-s solver: pressure and specific entropy as input pairs.
- h-s solver: specific enthalpy and entropy as input pairs.

3. COMPRESSIBLE FLOW RELATIONS AND COMPUTATIONAL FLOW SOLVERS

The expressions presented by Anderson (2003) to characterize the behavior of the quasi-one-dimensional steady flow in a converging-diverging nozzle are given by:

$$\rho_1 u_1 A_1 = \rho_2 u_2 A_2 \tag{13}$$

$$P_1 + \rho_1 u_1^2 = P_2 + \rho_2 u_2^2 \tag{14}$$

$$h_1 + u_1^2 = h_2 + u_2^2 \tag{15}$$

$$s_1 = s_2 \tag{16}$$

Equations (13), (14), and (15) are the mass, momentum and energy conservation ones. ρ is the density of the fluid, A is the transversal area of the nozzle, u is the flow speed and the subscripts 1 and 2 denote two arbitrary locations in the nozzle.

In the case of normal shock occurrence, Eqs. (13-15) may be used to calculate the conditions upstream and downstream the shock. When an isentropic expansion is just considered, the flow conditions are calculated by Eqs. (13), (15) and (16).

To obtain the flow properties distribution in the nozzle, the principal locations such as the throat and the normal shock location are determined implementing a series of Python solvers which satisfy the conservation equations.

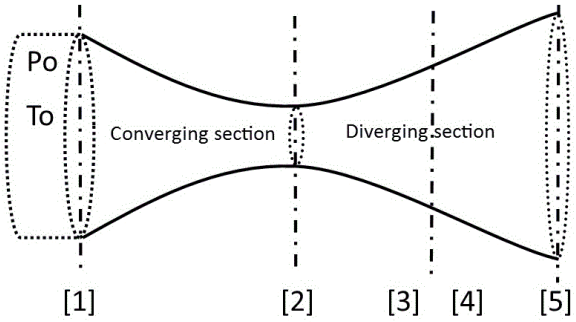

Figure 1: Principal nozzle locations.

In Figure. 1, the nomenclature for the nozzle locations is presented: [1] corresponds to the nozzle inlet, [2] the throat, [5] nozzle outlet, [3] and [4] upstream and downstream the normal shock, respectively, and Po, To, denote the total pressure and temperature at the nozzle inlet, respectively. In order to solve the principal locations of the nozzle in Fig. 1, four functions are coded in Python.

3.1 Throat solver

The throat solver returns the difference between the mass flow rate calculated at the nozzle inlet and throat by giving a guess of pressure at the throat. Its input parameters are: the mentioned guess value of the pressure, the nozzle inlet and throat areas, the enthalpy and entropy at the nozzle inlet.

The guess value of the pressure and the nozzle inlet entropy are given to the P-s thermodynamic solver to obtain the volume, enthalpy and speed of sound at the throat. The total enthalpy (h_o) at this location is calculated in Eq. (17):

$$h_{o[2]} = h_{[2]} + c_{[2]}^2/2 \tag{17}$$

Note that the speed of the flow is equal to the speed of sound at the throat. Thus, the mass flow rate at this location is determined by:

$$\dot{m}_{[2]} = \frac{A_{[2]} c_{[2]}}{V_{[2]}} \tag{18}$$

The speed and mass flow rate at the nozzle inlet, are obtained from Eqs. (19-20), respectively.

$$u_{[1]} = \sqrt{2\left(h_{o[2]} - h_{[1]}\right)} \tag{19}$$

$$\dot{m}_{[1]} = \frac{A_{[1]} c_{[1]}}{V_{[1]}} \tag{20}$$

Finally, the return value of this function may be written as:

$$y = \dot{m}_{[2]} - \dot{m}_{[1]} \tag{21}$$

3.2 Isentropic expansion solver

The isentropic expansion returns the difference of the mass flow rate between a reference location such as the nozzle throat shock and any point in the nozzle, when a guess value of pressure is given. It allows to determine the profile of the flow conditions along an isentropic expansion. The inputs of this function are: the guess value of pressure, the area that needs to be solved, the mass flow rate, the entropy and total energy ($h_{[ref]} + u^2_{[ref]}/2$) at the reference location.

$$s_{[i]} = s_{[ref]} \tag{22}$$

Where the subscripts $[i]$ and $[ref]$ denote the arbitrary and reference location at the nozzle. In the same manner as the throat function, the P-s thermodynamic solver is called, then the enthalpy and volume are obtained. The total enthalpy is determined by Eq. (23) at the reference location.

$$h_{o[ref]} = h_{[ref]} + u^2_{[ref]}/2 \tag{23}$$

Afterwards, the speed and mass flow rate at $[i]$ are obtained by applying Eqs. (19), and (20), the return value is the same as the throat solver Eq. (21).

3.3 Normal shock wave and shock location solver

When the flow conditions upstream the normal shock wave are known, the shock function returns the difference between the pressure and enthalpy obtained from guess values of pressure and temperature downstream the normal shock and those calculated from the mass, energy and momentum quantities upstream the shock.

The input parameters of the shock function are: the pressure and temperature guess values downstream the normal shock wave and three constants defined as:

$$K_{\dot{m}[3]} = u_{[3]}/V_{[3]} \tag{24}$$

$$K_{E[3]} = h_{[3]} + u^2_{[3]}/2 \tag{25}$$

$$K_{M[3]} = P_{[3]} + u_{[3]}/V_{[3]} \tag{26}$$

The constants given by Eqs. (24), (25) and (26) are the mass, energy and momentum quantities upstream the shock, respectively. The volume ($V_{[4]}$) and enthalpy ($h_{[4]}$) are calculated by giving the guess values of the pressure and temperature to the P-T solver. Then the speed downstream the normal shock is determined by:

$$u_{[4]} = k_{\dot{m}[3]} V_{[4]} \tag{27}$$

. The pressure ($P_{[4]f}$) and enthalpy ($h_{[4]f}$) downstream the normal shock wave are defined by Eqs. (28) and (29), respectively.

$$P_{[4]f} = K_{M[3]} - u^2_{[4]}/V_{[4]} \tag{28}$$

$$h_{[4]f} = K_{E[3]} - u^2_{[4]}/2 \tag{29}$$

Then the return value of this function may be written as:

$$y_0 = P^*_{[4]} - P_{[4]f} \tag{30}$$

$$y_1 = h_{[4]} - h_{[4]f} \tag{31}$$

Note that the return value is a vector in which its elements are determined by the subscripts 0 and 1, in Eq. (30) the pressure guess value is denoted by $P^*_{[4]}$.

Finally, another solver is coded to locate the normal shock wave, it returns the difference between an estimated outlet pressure ($P_{[5]}$) and the actual outlet pressure (P_{out}) which is an initial condition of the problem, it works in the following manner: it gives an arbitrary area of the normal shock wave in the divergent section of the nozzle, then the isentropic

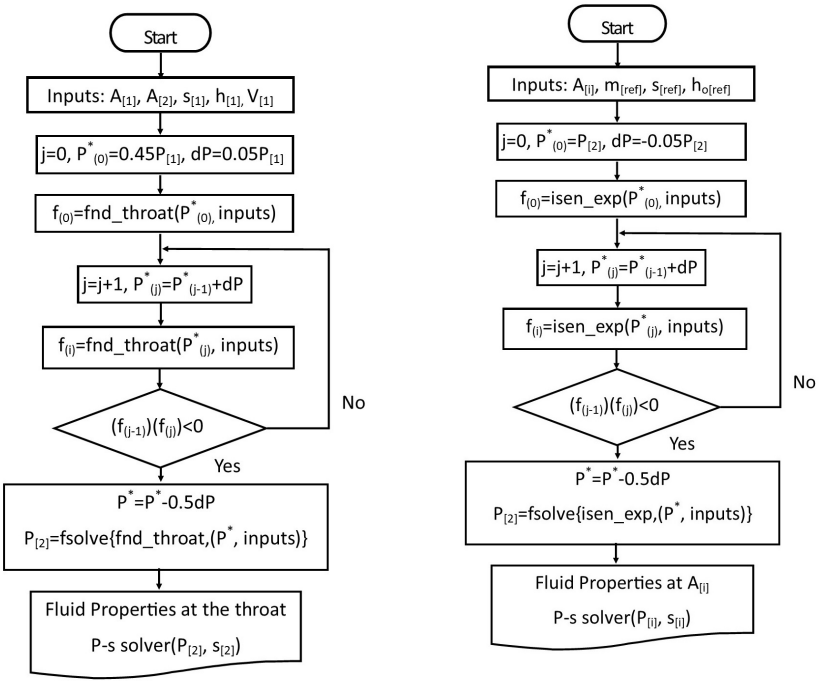

(a) (b)

Figure 2: (a) throat and (b) isentropic expansion algorithms.

expansion solver is called, using the nozzle throat as the reference location to obtain the conditions upstream the normal shock, the shock function is employed to obtain the flow properties downstream the normal shock, consequently, the isentropic expansion solver is called again, the reference state is fixed at downstream shock location and the outlet pressure is calculated. The return value of this function is expressed as:

$$y = P_{[5]} - P_{out} \tag{32}$$

As it is appreciated, the return values (y) of the functions treated in this section are differences, when they achieve the convergence criteria, the objective conditions are found.

Although, the solution of the isentropic expansion and throat function results in the pressure of the throat and of the $[i]$ location. The algorithms to find the throat and isentropic expansion pressures, are given in Fig. 2.

As it is observed in Fig. 2, the algorithms to obtain the solution of both functions are similar, they include the basis of root finding, looking for and interval in which the functions change of sign, then $fsolve$ from Scipy (Jones *et al.*, 2001) equation solvers is called, and the objective pressure is found.

When the pressure and entropy are known at any nozzle location, the other thermodynamic properties are obtained by calling the (P-s) solver. According to the normal shock function, it is solved using $fsolve$ directly, finally the bisection method is employed to obtain the shock location.

4. METASTABILITY AND HOMOGENEOUS NUCLEATION

4.1 Binodal and spinodal curves

The binodal curve, denotes the conditions in which two different phases coexist. In a general manner, it is defined as the point in which the chemical potential is equal for each phase for a pure substance or mixture. The expression to calculate the fugacity of the liquid and vapor phase for the PR EoS reported by Smith *et al.* (2006) is determined by:

$$\ln(f/P) = Z - 1 - \ln(Z - B) - (A/2.828)\ln\left(\frac{Z + (1+\sqrt{2})B}{Z + (1-\sqrt{2})B}\right) \tag{33}$$

Where f is the fugacity of the phase, it is calculated for the vapor and liquid by iterating with a pressure value at a fixed temperature, when the fugacity is equal for both phases at a certain pressure, that pressure and temperature correspond to the binodal curve.

It should be mentioned, that the spinodal curve establishes the limit of the metastable state, for cubic equations of state, it is obtained when the derivative of the pressure respect to the volume at constant temperature is zero. For the PR

EoS, this term may be expressed as:

$$\left(\frac{\partial P}{\partial V}\right)_T = T - \left(\frac{2a}{R}\right)\frac{(V+b)(V-b)^2}{(V^2+2bV-b^2)^2} = 0 \tag{34}$$

The binodal and spinodal curved are implemented using the PR EoS for carbon dioxide as it is presented in Fig. 3.

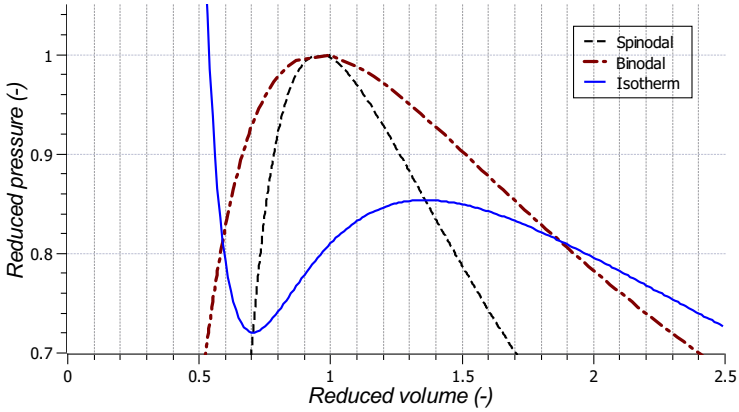

Figure 3: Binodal and spinodal curves for carbon dioxide implemented on the PR EoS

The isotherm in Fig. 3 corresponds to the reduced temperature of 0.97 (295 K), the zone delimited by the binodal and spinodal curve is known as the metastable region, where the phase change occurs for a non-equilibrium condensation process. The criteria for determining that phenomenon is given by the homogeneous nucleation theory.

4.2 Aspects of homogeneous nucleation

The homogeneous nucleation approach is taken that of Pandey (2014), which is based on the classical nucleation theory. The nucleation starts (formation nano-droplets particles) when the nucleation rate (J_{CL}) exceeds a critical value, the expression to calculate the nucleation rate is determined by:

$$J_{CL} = \frac{\alpha_c \rho_v^2}{C\rho_l}\sqrt{\frac{2\sigma}{\pi m^3}}\exp\left(\frac{-4\pi r^{*2}\sigma}{3k_b T_v}\right) \tag{35}$$

Where α_c is the condensation coefficient, its value is 0.1 for carbon dioxide (Bier *et al.*, 1990), ρ_v and ρ_l are the density of the vapor and liquid respectively, σ is the surface tension, m is the molecular mass of the carbon dioxide, r^* is the critical radius expressed in Eq. (37), C is a non isothermal correction factor given by Eq. (36), k_b is the Boltzmann constant and T_v is the vapor temperature.

$$C = 1 + 2\frac{\gamma-1}{\gamma+1}\frac{h_v - h_l}{RT_v}\left(\frac{h_v - h_l}{RT_v} - \frac{1}{2}\right) \tag{36}$$

$$r^* = \frac{2\sigma}{\rho_l R T_v Ln\,(S)} \tag{37}$$

Where $\gamma = c_p/c_v$ and S is the supersaturation ratio which determines the degree of the metastability of the fluid expansion.

$$S = \frac{P_v}{P_{eq}} \tag{38}$$

Where, P_v is the vapor pressure at T_v, P_{eq} is the saturation pressure at the mentioned local vapor temperature.

5. RESULTS AND DISCUSSION

The simulations were carried out using the geometry that of Arina (2004), which is expressed as:

$$A\,(x) = 2.5 + 3\left(\frac{x}{x_{th}} - 1.5\right)\left(\frac{x}{x_{th}}\right)^2 \qquad x \le x_{th} \tag{39}$$

$$A(x) = 3.5 - \frac{x}{x_{th}}\left\{6 - 4\frac{x}{x_{th}} + \left(\frac{x}{x_{th}}\right)^2\right\} \quad x \geq x_{th} \tag{40}$$

Where x_{th} is the throat location, it has been positioned at x =5 cm and its area is 8E-06 m^2, note that the inlet (x = 0 cm) and outlet (x = 10 cm) area ratio to the throat are 2.5 and 1.5, respectively. The procedure to obtain the thermodynamic and physical property profiles along the nozzle implements the procedures discussed in sections 2 and 3. It starts finding the flow conditions at the principal nozzle locations, then the isentropic solver obtains the solution for any point of the nozzle where the isentropic condition is satisfied. The nozzle geometry was divided in 270 elements (uniform mesh) for both EoS. It is important to clarify that the present work is a different CFD approach, the conservation equations are treated as balanced quantities Eqs. (13-14) instead of differential equations, and the convergence is achieved when the return values (y) are less than 1.8E-06.

5.1 Normal shock wave Location

According to the normal shock wave location, two simulations using the VdW EoS are carried out. The input conditions for the first simulation are the nozzle inlet temperature and pressure of 288 K and 1 bar, the actual outlet (P_{out}) pressure is fixed at 0.83049 bar, and nitrogen as working fluid. The obtained results are listed in Tab.1 and the pressure profile is displayed in Fig. 4.

Table 1: Thermodynamic properties and Mach number at the main nozzle locations ($T_{[1]}$=288 K and $P_{[1]}$=1 bar).

L	Temperature (K)	Pressure (bar)	Density (kg/m-3)	Mach (-)	Total temperature (K)	Total pressure (bar)
1	288	1	1.17076	0.239518	291.29	1.04069
2	243.029	0.550456	0.763719	1	291.29	1.04069
3	201.611	0.284595	0.475942	1.49961	291.29	1.04069
4	265.346	0.697513	0.88631	0.700923	291.27	0.967833
5	278.852	0.83049	1.00416	0.473053	291.27	0.967833

Note that the total temperature remains constant (Tab.1) upstream and downstream the normal shock, which is a characteristic of ideal gas behavior. The maximum Mach number ($M = u/c$) achieved is 1.49 upstream the shock, the pressure and temperature drop during the isentropic expansion from the nozzle inlet to upstream the normal shock corresponds to 71 and 30 percent respect to the inlet ones. The pressure profile is compared to that of Arina (2004) in Fig. 4.

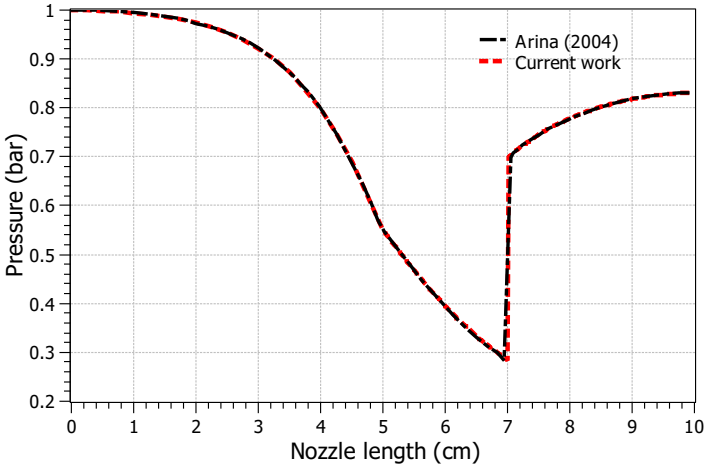

Figure 4: Pressure profile of nitrogen at ideal conditions.

As it is appreciated in Fig. 4 the normal shock location occurs at x= 7 cm, for both solutions. The pressure profile obtained agreed very well with the compared reference.

To test the capacity of convergence of the algorithm, the final simulation with the VdW EoS is carried out close to the critical point of carbon dioxide, at 98 percent of the critical pressure, the temperature is fixed at its critical condition at the nozzle inlet and the actual outlet pressure is $0.83049 P_{[1]}$. The results for the principal nozzle locations are reported in Tab. 2, the density ratio profile $\rho/\rho_{[1]}$ is also compared to that of Arina (2004) as it is appreciated in Fig. 5.

The temperature and pressure drop from the nozzle inlet to upstream the normal shock wave are 31 and 66 percent respect to the inlet ones, The pressure and temperature recuperation at the normal shock wave are 22 and 40 percent

Table 2: Thermodynamic properties and Mach number at the main nozzle locations close to the critical carbon dioxide conditions.

L	Temperature (K)	Pressure (bar)	Density (kg/m-3)	Mach (-)	Total temperature (K)	Total pressure (bar)
1	304.128	72.5926	264.253	0.232231	307.256	75.057
2	258.595	45.0513	171.483	1	307.256	75.057
3	208.271	24.2175	95.5567	1.45749	307.256	75.057
4	274.985	53.2988	195.771	0.697641	299.703	68.9306
5	286.804	60.2875	219.271	0.493418	299.703	68.9306

respectively, and the maximum Mach number attained is 1.45.

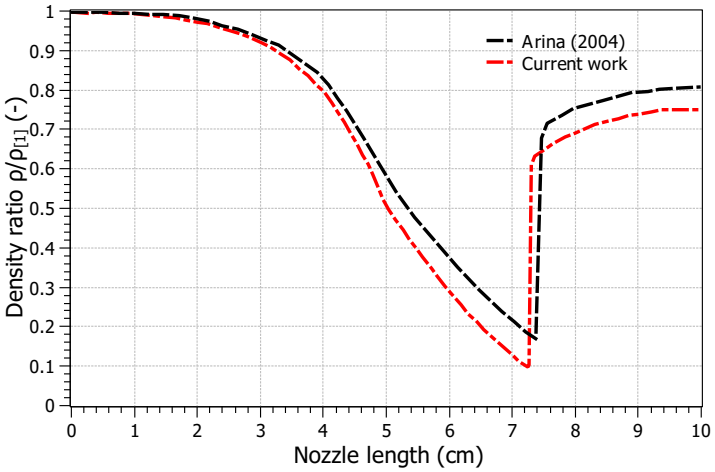

Figure 5: Profile of density ratio for carbon dioxide close to critical conditions

According to the density ratio profile presented in Fig. 5, the normal shock wave is located about at x=7.24 cm for both solutions, the results agreed well from the nozzle inlet to the throat, the maximum deviation is 7 percent which finds upstream the normal shock.

5.2 Wilson line and condensation shock location

The Wilson line defined as the limit of supersaturation of a vapor, where the onset of nucleation occurs (Pandey, 2014), is built for carbon dioxide, and also an isentropic expansion is carried out employing the PR EoS.

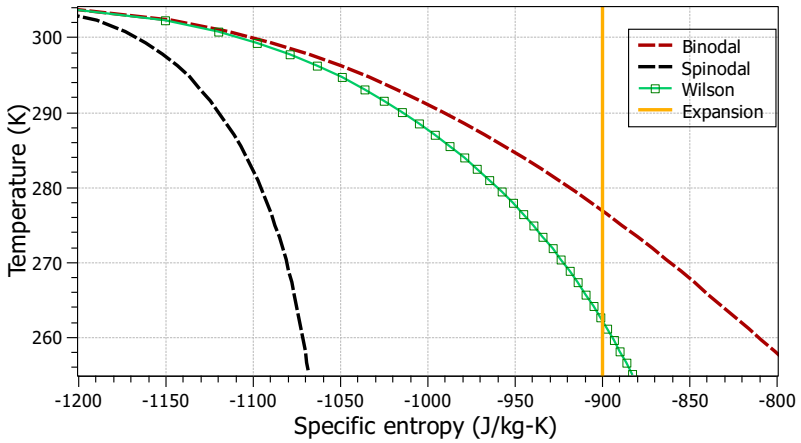

Figure 6: Binodal and spinodal curves for carbon dioxide implemented on the PR EoS.

To calculate the Wilson curve for carbon dioxide in Fig. 6, Eqs. (32-35) are employed and the critical J_{CL} is assumed as 10^{30} m^{-3} s^{-1} to guarantee the minimum vapor quality of 0.95 when the reduce temperature finds far from the critical point (Korpela, 2019). Bier *et al.* (1990) carried out experimental tests to determine the nucleation rate and suggest the value of 10^{20} m^{-3} s^{-1}. However, the purpose of this section is to develop the methodology to locate the condensation shock, which can be applied to accurate equations of state such as Span and Wagner (1996) EoS in future works.

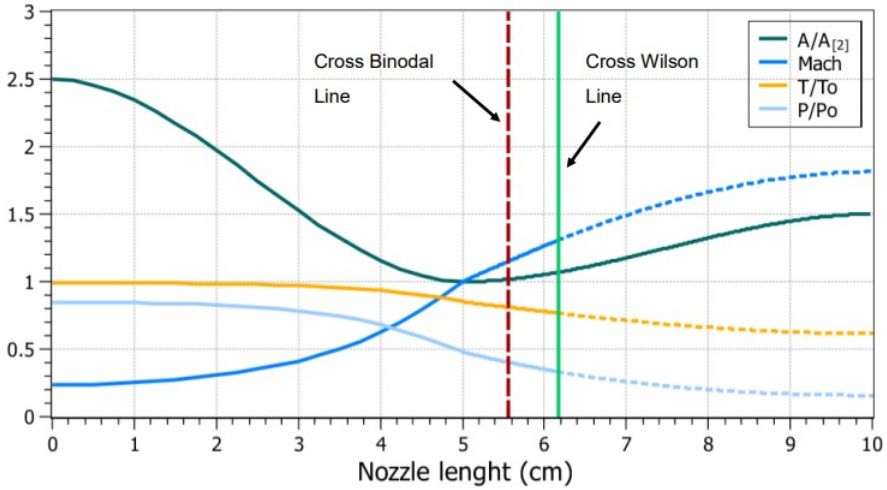

Figure 7: Isentropic expansion for carbon dioxide at Po=85 bar, To= 342.23 K.

Finally, the simulation of the isentropic expansion is carried out, considering an inlet total temperature and pressure of 342.23 K and 85 bar. The Wilson point where the jump conditions of the condensation shock must be implemented, is presented in Fig. 7. The profiles of the temperature (T/To), pressure (P/Po) and area ratios ($A/A_{[2]}$), same as the Mach number along the nozzle are also appreciated in this figure. It should be pointed out that the purpose of this section is to locate the condensation shock during an isentropic expansion, not to characterize the liquid phase formation and the two-phase flow behavior downstream the condensation shock.

As it is observed in Fig. 7, the temperature and pressure ratios, and Mach number are represented by continuous curves upstream the condensation shock (x= 6.18 cm) and dashed ones downstream, due to the fact that the single-phase implemented model does not have validity in this region of the nozzle (from x=6.18 to 10 cm). In Fig. 6, it is also appreciated when the fluid isentropic expansion meets the binodal and Wilson curve in a T-s diagram.

6. CONCLUSIONS

A quasi one-dimensional model was implemented in a Python code library, using two classical cubic equations-of-state (Van der Waals and Peng-Robinson) departing from the residual thermodynamic property theory, the conservation equations were solved which allowed to obtain the normal shock wave employing the Van der Waals EoS, and the condensation shock location with the Peng-Robinson equation by applying the main concepts of the classical nucleation theory.

From a general point of view, compressible flow behavior in converging-diverging nozzles was determined far from ideal conditions and the methodology for locating the phase-change in a supersonic nozzle was achieved. The results agreed well with the numerical data available on the reviewed literature in ideal and close to the critical conditions.

This work will be extended to predict the pressure, nucleation rate, number of droplets profiles for pure substance and gas-mixtures during the condensation process in supersonic nozzle flows.

7. ACKNOWLEDGEMENTS

The authors would like to thank the sponsorship of Shell and FAPESP through the “Research Centre for Gas Innovation - RCGI” (FAPESP Proc. 2014/50279-4), hosted by the University of Sao Paulo, and the strategic importance of the support given by ANP (Brazil’s National Oil, Natural Gas and Biofuels Agency) through the $R\&D$ levy regulation. The last author thanks CNPq for the research scholarship..

8. REFERENCES

Anderson, J., 2003. *Modern Compressible Flow With Historical Perspective*. Mc Graw Hill, third edit edition.

Arina, R., 2004. “Numerical simulation of near-critical fluids”. *Appl. Numer. Math.*, Vol. 51, No. 4 SPEC. ISS., pp. 409–426. ISSN 01689274. doi:10.1016/j.apnum.2004.06.002.

Bier, K., Ehrler, F. and Theis, G., 1990. “Spontaneous Condensation in Stationary Nozzle Flow of Carbon Dioxide in a Wide Range of Density”. In *Adiabatic Waves Liq. Syst.* Springer Berlin Heidelberg, pp. 129–141.

Haghighi, M., Abedinzadegan Abdi, M. and Hawboldt, K., 2013. “Natural Gas Dehydration Using Supersonic Separators with a Novel Design”. *Offshore Technol. Conf.*, , No. 2013. doi:10.4043/23974-MS. URL `http://www.onepetro.org/doi/10.4043/23974-MS`.

Jones, E., Oliphant, T., Peterson, P. *et al.*, 2001. “SciPy: Open source scientific tools for Python”. URL

http://www.scipy.org/. [Online; accessed <today>].

Korpela, S.A., 2019. *PRINCIPLES OF TURBOMACHINERY*. John Wiley & Sons, Ltd, Ohio, 2nd edition. ISBN 9780470536728.

Liu, X., Liu, Z. and Li, Y., 2014. "Investigation on Separation Efficiency in Supersonic Separator with Gas-Droplet Flow Based on DPM Approach". *Sep. Sci. Technol.*, Vol. 49, No. 17, pp. 2603–2612. ISSN 15205754. doi:10.1080/01496395.2014.938755. URL http://dx.doi.org/10.1080/01496395.2014.938755 https://doi.org/10.1080/01496395.2014.938755.

Niknam, P.H., Mortaheb, H.R. and Mokhtarani, B., 2017. "Optimization of dehydration process to improve stability and efficiency of supersonic separation". *J. Nat. Gas Sci. Eng.*, Vol. 43, pp. 90–95. ISSN 18755100. doi:10.1016/j.jngse.2017.03.017. URL http://dx.doi.org/10.1016/j.jngse.2017.03.017.

Niknam, P.H., Mortaheb, H.R. and Mokhtarani, B., 2018. "Dehydration of low-pressure gas using supersonic separation: Experimental investigation and CFD analysis". *J. Nat. Gas Sci. Eng.*, Vol. 52, No. November 2017, pp. 202–214. ISSN 18755100. doi:10.1016/j.jngse.2017.12.007. URL https://doi.org/10.1016/j.jngse.2017.12.007.

Oliphant, T., 2006. "NumPy: A guide to NumPy". USA: Trelgol Publishing. URL http://www.numpy.org/. [Online; accessed <today>].

Pandey, A., 2014. *Numerical Modeling of Non- Equilibrium Condensing Steam Flows*. Ph.D. thesis, Delft University of Technology.

Pratt, R., 2001. "THERMODYNAMIC PROPERTIES INVOLVING DERIVATIVES:Using the Peng-Robinson Equation of State". *Chem. Eng. Educ.*, , No. 35, pp. 112–139.

Restrepo, J. and Simões-Moreira, J.R., 2019. "OPERATIONAL BEHAVIOUR OF SUPERSONIC SEPARATORS FOR REAL GAS MIXTURES OF METHANE AND CARBON DIOXIDE, FROM THE HOMOGENEOUS NUCLEATION POINT OF VIEW." *Proc. ASME 2019 38th Int. Conf. Ocean. Offshore Arct. Eng.*, pp. 1–7.

Rossum, G., 1995. "Python reference manual". Technical report, Amsterdam, The Netherlands, The Netherlands.

Smith, J., Van Ness, H.C. and Abbott, M., 2006. *Introduction to Chemical Engineering Thermodynamics*. McGraw-Hill, 7th edition. ISBN 0073104450.

Span, R. and Wagner, W., 1996. "A New Equation of State for Carbon Dioxide Covering the Fluid Region from the Triple-Point Temperature to 1100 K at Pressures up to 800 MPa". *J. Phys. Chem. Ref. Data*, Vol. 25, No. 6, pp. 1509–1596. ISSN 0047-2689. doi:10.1063/1.555991. URL http://aip.scitation.org/doi/10.1063/1.555991.

9. RESPONSIBILITY NOTICE

The author(s) is (are) the only responsible for the printed material included in this paper.